AXISYMMETRIC DYNAMIC BEHAVIOUR
OF THIN OBLATE SHELLS

By
Ahmed A. Al – Rajihy ; Ala M. Hussein Al – Jessany
Nawal H. Al – Raheimy
College of Engineering,
Babylon University

ABSTRACT

This paper presents a theoretical investigation of the axisymmetric free vibrations of an isotropic thin oblate spheroid shell. The analysis depends on the Rayliegh – Ritz's method. The non – shallow shell theory is used for the analysis. The analysis based on considering the oblate spheroid as a continuous system constructed from two spherical shell elements matched at the continuous boundaries.

Throughout the results, it is shown that when the eccentricity reaches zero, an exact thin sphere solution is emerged and when the eccentricity equals one an exact thin circular plate solution is emerged. Therefore, the eccentricity of an oblate shell at medium value lies between these two values.

It was found that the Rayleigh – Ritz's method is suitable for all eccentricities, while the literature showed that the Rayleigh's method is suitable for eccentricities less than 0.6.

الخلاصة

يتناول هذا البحث دراسة نظرية للاهتزازات الحرة للقشريات نحيفة الجدران شبه البيضوية الشكل المتناظرة المحور والمتشابهة الخواص في جميع الاتجاهات. التحليل النظري يعتمد على طريقة (Rayliegh – Ritz) وقد تم استخدام (نظرية القشريات العميقة) في التحليل. هذه التقنيه مبنية على أساس القشرية الشبه بيظويه كمنظومة مستمرة مركبه من قشريتين نصف كرويتين متناظرتين على طول حدودها المستمرة.

من خلال النتائج، تبين بأنه عندما تصل اللامركزية إلى الصفر يكون ظاهر للعيان بالضبط حل لقشرية نحيفة كروية الشكل وعندما تكون اللامركزية مساوية إلى الواحد يكون ظاهر للعيان بالضبط حل لصفيحة نحيفة دائرية الشكل، وبناءً عليه فان اللامركزية للشكل شبه البيضوي يقع عند قيمة متوسطة ما بين تلك القيمتين.

وجد إنّ طريقة (Ritz – Rayliegh) ملائمة لكل قيم اللامركزية، بينما أظهرت البحوث السابقة إن طريقة (Rayliegh) تكون ملائمة لقيم من اللامركزية اقل من (0.6).

KEY WORDS

Oblate, Spheroid, Thin shells, Axisymmetric spheroid

LIST OF SYMBOLS

a	Major semi – axis of an oblate spheroid shell.
b	Minor semi – axis of an oblate spheroid shell.
E	Young's modulus of elasticity (GN/m^2).
e	Eccentricity ratio.
h	Shell thickness (mm).
$P_n(x)$	Legendre function of the first kind.
$P'_n(x)$	First derivative of the Legendre function of the first kind.
$P''_n(x)$	Second derivative of the Legendre function of the first kind.
R_r	Effective radius.
R_Φ , R_θ	Principal radii of curvatures of an oblate spheroid.
U_Φ	Tangential displacement mode.
u_Φ	Tangential displacement of points on shell middle surface.
W	Transverse displacement mode.
w	Transverse displacement of points on shell middle surface.
$\epsilon_\Phi, \epsilon_\theta, \epsilon_r$	Strains
Φ'	Inclination angle of an oblate spheroid.
Φ	Inclination angle of a spherical shell model.
Φ_o	Opening angle of the approximate spherical shell.
λ	Non – dimensional frequency parameter $((\rho / E)^{1/2} \omega.a)$. (used for oblate spheroid shells)
θ	Angle of rotation in the meridian direction.
ρ	Density (kg/m^3).
Ω	Non – dimensional frequency parameter $((\rho / E)^{1/2} \omega.R)$. (used for spherical shells)
ω	Circular frequency (rad / sec).

INTRODUCTION

Oblate spheroid shell is defined as the locus surface resulting by rotating an ellipse around its minor axis. This type of shells has many practical applications such as; the tanks of liquid oxygen used in space vehicles, the housing of the early – warning scanner of the airborne warning and control system aircraft (AWACS) and others. These applications may cause dynamic problems to these shells. One of the very important dynamic problems is the resonance. Therefore the free vibration of such shells may be studied to present the resonant problem.

The dynamics of oblate spheroid shells, like other types of shells and structures, has received a considerable attention in the literature, partly because of the necessity during the

design stage of such shells, and partly because it is an interesting fundamental problem in applied mechanics.

Baker, 1969 presented a detailed study of the theory of free, axisymmetric vibration of thin elastic spherical shell and demonstrate by experiments that the normal modes of vibration predicted do exist. The theory predicts the existence of two infinite sets of normal modes, one of which is bounded in frequency and the other unbounded. The first four modes in each set are identified by experiments on a small steel shell.

As for the oblate spheroid shells, **Penzes** and **Burgin, 1965** were the first to solve the problem of the free vibrations of thin isotropic oblate spheroid shells by Galerkin's method using membrane theory and harmonic axisymmetric motion. It was shown that Galerkin's method of solution for the oblate spheroid shell yields the exact solution for the closed spherical shell as the eccentricity of the oblate spheroid shell approaches zero.

Penzes, 1969 extended the solution of the above reference to include thin orthotropic oblate spheroid shells. He used the same assumptions and equations of motion in the above reference except that the principal direction of the elastic compliances was assumed to be along parallel of latitude and along meridian. Both of the spheroid and spherical shells were investigated with various orthotropic constants. The discussion was restricted to the axially symmetric torsionless motion of shells.

Tavakoli and **Singh, 1989** used a substructure synthesis method based on state space mathematics for the eigen – solution of axisymmetric joined / hermitic thin shell structures. The authors applied the state space method to the cylindrical, conical, spherical, and toroidal shells. They compared their results with results obtained previously for the same shells by applying the theoretical analysis and the finite element method. The state space method has strengths lies primarily in its ability to join substructures and match the boundary variables comprehensively.

Fawaz, 1990 in his M.Sc. thesis the Rayliegh variation method was used to obtain natural frequencies and mode shapes of axisymmetric vibrations of thin elastic oblate spheroidal shells and presents the results theoretically and experimentally. He showed that the Rayliegh's method was found to be suitable only for oblate shells with eccentricities less than 0.6.

Chang and **Demkowicz, 1998** studied the stability analysis of multilayered vibrating viscoelastic spheres, both in vacuo and in an acoustical fluid. The analysis was done by investigating the effect of viscoelastic damping on the (continuous) Ladyzenskaya – Babuska – Brezzi (LBB) constants for the related boundary – value problems. The sphere is modeled using both 3–D viscoelasticity and the Kirchho – Love shell theory.

In the paper presented by **Antoine Chaign et. al. 2002,** linear and nonlinear vibrations of shallow spherical shells with free edge are investigated experimentally and numerically and compared to previous studies on percussion instruments such as gongs. The preliminary bases of a suitable analytical model are given. Identification of excited modes is achieved through systematic comparisons between spatial numerical results obtained from a finite element modeling, and spectral information's derived from experiments.

In this paper the free vibration characteristics of a thin elastic oblate spheroid shell will be examined using Raylrigh – Ritz's method to examine its validity for this type of shells.

THEORETICAL ANALYSIS

The review of literature reveals that even though the differential equations of motion for general shell of revolution are well spelt out, nevertheless, the formulation of these equations for oblate spheroidal shells are not available. Hence, an approximate energy approach will be presented in section (2.1) of this paper.

<u>The Rayleigh – Ritz's Energy Method</u>

The Rayliegh – Ritz's method is an extension of Rayliegh's quotient which can be used for more complex elastic bodies and helps to determine the natural frequencies and their associated mode shapes with general boundary conditions in an approximate form. This method is essentially statements on the ratio of potential energy to the kinetic energy. Physically, it makes sense that this ratio is related to the frequency of oscillation [Hayam]. At the natural frequency (ω), and assuming separation of variables, the shell displacements may be written in the following forms [**Penzes, 1969**] :-

$$w(\Phi', t) = W(\Phi') \cdot e^{i\omega t}$$

and . . . (1)

$$u_\Phi(\Phi', t) = U_\Phi(\Phi') \cdot e^{i\omega t}$$

Substituting these in the strain energy expression gives :

$$U = \int_{-h/2}^{h/2} \int_0^{2\pi} \int_0^{2\pi} \frac{1}{2} [\sigma_{\Phi'} \; \epsilon'_{\Phi'} + \sigma_\theta \; \epsilon'_\theta] \, R_\Phi \, R_\theta \sin \Phi' \, d\Phi \, d\theta \, dz \qquad \ldots (2)$$

where,

$$\sigma_{\Phi'} = \frac{E}{(1-v^2)} [\, \epsilon'_{\Phi'} + \upsilon \, \epsilon'_\theta \,] \quad , \quad \sigma_\theta = \frac{E}{(1-v^2)} [\, \epsilon'_\theta + \upsilon \, \epsilon'_{\Phi'}]$$

and . . . (3)

$$\epsilon'_{\Phi'} = \epsilon^\circ_\Phi + Z \, K_\Phi \qquad , \quad \epsilon'_\theta = \epsilon^\circ_\theta + Z \, K_\theta$$

An expression for the maximum potential energy [U_{max}] may be obtained upon taking $e^{i\omega t}$ to be unity and applying the appropriate expressions for σ_Φ, σ_θ, ϵ'_θ and ϵ'_θ, gives;

$$U_{max} = \frac{Eh}{2(1-\upsilon^2)} \int_0^{2\pi} \int_0^{2\pi} \{ \frac{h^2}{12} \left[\frac{1}{R_\Phi^2} \left[\frac{\partial}{\partial\Phi'} \left[\frac{U_\Phi}{R_\Phi} - \frac{\partial W}{R_\Phi \partial\Phi'} \right] \right]^2 \right. $$

$$+ \frac{\cos^2\Phi'}{R_\Phi^2 R_\theta^2 \sin^2\Phi'} \left[U_\Phi - \frac{\partial W}{\partial\Phi'} \right]^2 + 2\upsilon \frac{\cos\Phi'}{R_\theta R_\Phi^2 \sin\Phi'} \left[U_\Phi - \frac{\partial W}{\partial\Phi'} \right] .$$

$$\left. . \frac{\partial}{\partial\Phi'} \left[\frac{U_\Phi}{R_\Phi} - \frac{\partial W}{R_\Phi \partial\Phi'} \right] \right] + \frac{1}{R_\Phi^2} \left[\frac{\partial U_\Phi}{\partial\Phi'} + W \right]^2$$

$$+ \frac{1}{(R_\theta \sin\Phi')^2} (U_\Phi \cos\Phi' + W \sin\Phi')^2$$

$$+ \frac{2\upsilon}{R_\theta R_\Phi \sin\Phi'} \left[\frac{\partial U_\Phi}{\partial\Phi'} + W \right] .(U_\Phi \cos\Phi' + W \sin\Phi') \}.$$

$$R_\Phi R \sin\Phi' d\Phi' d\theta \qquad \qquad \qquad \qquad \qquad \dots (4)$$

The kinetic energy expression is :

$$K = \int_{-h/2}^{h/2} \int_0^{2\pi} \int_0^{2\pi} \frac{1}{2} \rho \left[\left[\frac{\partial U_\Phi}{\partial t} \right]^2 + \left[\frac{\partial W}{\partial t} \right]^2 \right] R_\Phi R_\theta \sin\Phi' d\Phi' d\theta \, dz \qquad \dots (5)$$

After integrating with respect to (z) and substituting for the appropriate   expressions, the maximum kinetic energy will take the form:

$$K_{max} = \frac{\omega^2 \rho h}{2} \int_0^{2\pi} \int_0^{2\pi} (U_\Phi^2 + W^2) R_\Phi R_\theta \sin\Phi' d\Phi' d\theta \qquad \dots (6)$$

The kinetic energy for $\omega=1$ rad/sec is customarily define as K*max and therefore,

$$K_{max} = \omega K*max$$

For a system with no dissipation losses, as those due to friction or damping, the maximum potential energy equals the maximum kinetic energy, i. e.

$$U_{max} = \omega K*max$$

Equating the maximum kinetic energy to the maximum potential energy, an expression for the natural frequency may be written as :

$$U_{max} = K_{max}$$

or;

$$\omega_r^2 = \frac{U_{max}}{K_{max}} = \frac{N}{D} \qquad\qquad r = 1, 2, 3, \ldots, n \qquad\qquad \ldots (7)$$

where N and D represent the equations in the numerator and denominator, respectively. Following the procedure of Rayleigh − Ritz's method, the radial (or transverse) and tangential displacements can be written in power series form as :

$$w(\Phi') = \sum_{i=1}^{n} a_i . W_i(\Phi') \qquad , \qquad u_\Phi(\Phi') = \sum_{i=1}^{n} b_i . U_{\Phi_i}(\Phi') \qquad\qquad \ldots (8)$$

where a_i and b_i are coefficients to be determined. The functions $w(\Phi')$, $u_\Phi(\Phi')$ satisfy all the geometry boundary conditions of the system, i.e. along the matching region between the halves of the spheroid shells. Equation (7) is an exact expression for the frequency according to Rayleigh quotient. In order to use the procedure of Rayleigh − Ritz's method, equation (8) is substituted into equation (4) and (6), then the results is used in equation (7).

Now substituting equation (8) into equations (4) and (6), and after some mathematical manipulations, the following equation will result;

$$\omega_r^2 = \frac{\alpha}{\Psi} = \frac{N}{D} \qquad\qquad r = 1, 2, 3, \ldots, n \qquad\qquad \ldots (9)$$

where,

$$
\begin{aligned}
\alpha = \sum_{i=1}^{n} \sum_{j=1}^{n} c_i c_j \frac{E h \pi}{(1-\upsilon^2)} \int_0^{2\pi} \Big\{ & \frac{h^2}{12 R_\Phi^4} \big[U'_{\Phi i} U_{\Phi j}' - 2 U_{\Phi i}' W_i'' + W_i'' W_j'' \big] \sin\Phi' \\
& + \frac{\upsilon h^2}{6 R_\theta R_\Phi^3} \big[U_{\Phi i} U_{\Phi i}' - U_{\Phi i} W_i'' - U_{\Phi i}' W_i' + W_i' W_i'' \big] \cos\Phi' \\
& + \frac{h^2}{12 R_\Phi^2 R_\theta^2} \big[U_{\Phi i} U_{\Phi j} - 2 U_{\Phi i} W_i' + W_i' W_j' \big] \frac{\cos^2\Phi'}{\sin\Phi'} \\
& + \frac{1}{R_\Phi^2} \big[U_{\Phi i}' U_{\Phi j}' + 2 U_{\Phi i}' W_i + W_i W_j \big] \sin\Phi' \\
& + \frac{1}{R_\theta^2} \Big[U_{\Phi i} U_{\Phi j} \frac{\cos^2\Phi'}{\sin\Phi'} + 2 U_{\Phi i} W_i \cos\Phi' + W_i W_j \sin\Phi' \Big] \\
& + \frac{2\upsilon}{R_\Phi R_\theta} \big[U_{\Phi i} U_{\Phi i}' \cos\Phi' + U_{\Phi i}' W_i \sin\Phi' + U_{\Phi i} W_i \cos\Phi' + W_i W_i \sin\Phi' \big] \Big\}. \\
& . R_\Phi R_\theta \, d\Phi' \qquad\qquad \ldots (9a)
\end{aligned}
$$

$$\Psi = \sum_{i=1}^{n} \sum_{j=1}^{n} c_i c_j \int_0^{2\pi} \rho h \pi \big[U_i U_j + W_i W_j \big] R_\Phi R_\theta \sin\Phi' \, d\Phi' \qquad\qquad \ldots (9b) \qquad \text{whe}$$

re, c_i's , c_j's are equiponderate a_i , b_i , a_j , and b_j after mathematical processes and some

simplified and arrangement [**Nawal, 2005**].

where, $\sum_{i=1}^{n} \sum_{j=1}^{n} c_i c_j = \sum_{i=1}^{n} \sum_{j=1}^{n} \big(a_i a_j + b_i b_j + a_i a_i + b_i b_j - a_i b_i \big)$

An n – term finite sum leads to the estimation of the first frequencies.   Equations (9a) and (9b) give the physical properties of the shell from the stiffness and mass distribution point of view. The stiffness and mass of the shell are given by the following two equations respectively:

$$
k_{ij} = \frac{E h \pi}{(1-\upsilon^2)} \int_0^{2\pi} \frac{h^2}{12 R_\Phi^4} \{ \left[U_{\Phi i}{}' \, U_{\Phi j}{}' -2U_{\Phi i}{}' W_i{}'' + W_i{}'' W_j{}'' \right] \sin \Phi'
$$

$$
+\frac{\upsilon h^2}{6 R_\theta R_\Phi^3} \left[U_{\Phi i} U_{\Phi i}{}' - U_{\Phi i} W_i{}'' - U_{\Phi i}{}' W_i{}' + W_i{}' W_i{}'' \right] \cos \Phi'
$$

$$
+\frac{h^2}{12 R_\Phi^2 R_\theta^2} \left[U_{\Phi i} U_{\Phi j} - 2U_{\Phi i} W_i{}' + W_i{}' W_j \right] \frac{\cos^2 \Phi'}{\sin \Phi'}
$$

$$
+\frac{1}{R_\Phi^2} \left[U_{\Phi i}{}' U_{\Phi j}{}' + 2U_{\Phi i}{}' W_j + W_i \, W_j \right] \sin \Phi'
$$

$$
+\frac{1}{R_\theta^2} \left[U_{\Phi i} U_{\Phi j} \frac{\cos^2 \Phi'}{\sin \Phi'} + 2U_{\Phi i} W_i \cos \Phi' + W_i W_j \sin \Phi' \right]
$$

$$
+\frac{2\upsilon}{R_\Phi R_\theta} \left[U_{\Phi i} U_{\Phi i}{}' \cos \Phi' + U_{\Phi i}{}' W_i \sin \Phi' + U_{\Phi i} W_i \cos \Phi' + W_i W_i \sin \Phi' \right] \}.
$$

$$
. R_\Phi R_\theta \, d\Phi' \qquad \qquad ... (10)
$$

where primes denote differentiation with respect to Φ'.

and

$$
m_{ij} = \int_0^{2\pi} \rho h \pi \left[U_i U_j + W_i W_j \right] R_\Phi R_\theta \sin \Phi' d\Phi' \qquad \qquad ... (11)
$$

Then

$$
\omega_r{}^2 = \frac{N}{D} = \frac{\sum_{i=1}^n \sum_{j=1}^n c_i c_j \, k_{ij}}{\sum_{i=1}^n \sum_{j=1}^n c_i c_j m_{ij}} \qquad \qquad ... (12)
$$

In order to minimize the approximate value, which is given by equation (12), it should be differentiation with respect to c_i and equating the resulting expression to zero, that is :

$$
\frac{\partial}{\partial c_i} \left(\frac{N}{D} \right) = \frac{D \, \partial N / \partial c_i - N \, \partial D / \partial c_i}{D^2} = 0 \qquad i = 1, 2, 3, ..., n \qquad \qquad ... (13)
$$

The conversional way in which this equation can equal zero is if the numerator equals zero, since D is never equal to zero. The numerator can be written in a more useful form as :

$$\frac{\partial N}{\partial c_i} - \frac{N}{D}\frac{\partial D}{\partial c_i} = 0, \qquad i = 1, 2, \ldots, n \qquad \ldots (14)$$

It is as given by equation (7) $\omega_r^2 = N / D$, and n is the number of terms in the approximate solution. The infinite degrees of freedom system has been replaced by an n degrees of freedom system. Therefore, Equation (14) can be written in general matrix notation as :

$$\left[\{K\} - \omega^2\{M\}\right]\{c\} = \{0\} \qquad \ldots (15)$$

Since i can be taken as 1, 2,3,… the evaluation of this determinant provides the estimation of the first two natural frequencies ω_1^2 and ω_2^2. Since we have used a two–term approximate solution, it results in a two degrees of freedom approximated system.

In the present work, and adopting the same argument of [**Penzes and Burgin,1965**] that the mode shapes of a spherical shell satisfies the boundary conditions of an oblate spheroid shell, the assumed mode shapes were chosen to represent the first two modes of a closed spherical shell.

Engineering Model By Non – Shallow Shell Theory :

The problem of vibration of oblate spheroid shells will be treated by an engineering modeling approach where the oblate spheroid shell is modeled as a structure composed of two spherical shells joined rigidly at their ends. Centers of curvature of the two spherical shell elements fall along the minor axis of the proposed oblate spheroid [see Fig. (1) for details].

Such approximation is not far from reality, as the oblate spheroidal tanks are produced by joining, either by welding or riveting, two spherical shell elements through a toroidal shell element.

The effective radius (R_r) of the spherical shell model represents the radius of curvature at the apex of the shell. This radius can be obtained from the geometrical relation [**Penzes, 1965**].

$$R_\Phi = \frac{a(1-e^2)}{(1-e^2\cos^2\Phi')^{3/2}} \qquad \ldots (16)$$

Setting (Φ') to zero results the radius of the shell at the apex as:

$$R_r = \frac{a}{(1-e^2)^{1/2}} \qquad \ldots (17)$$

where,

$e = \left[1 - \frac{b^2}{a^2}\right]^{\frac{1}{2}}$, a and b represent the major axis and minor axis respectively.

e = 0 for sphere   ,   e = 1 for plate.

An approximate opening angle (Φ_0) may be obtained by using the following formula:

$$\Phi_o = \cos^{-1} \frac{R_r - b}{R_r} \qquad \qquad \dots (18)$$

Figures (2) and (3) show the values of the effective radius and opening angle versus the eccentricity respectively.
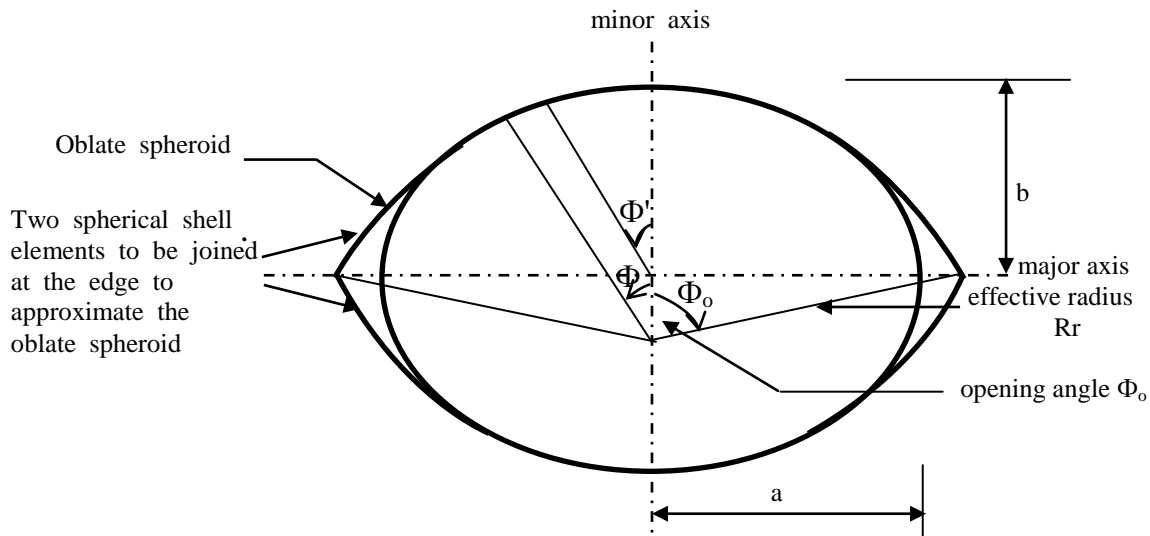

Fig. (1): An oblate spheroid and its approximate of two spherical shell elements joined at the edge.

RESULTS AND DISCUSSION:

The theoretical results and the available experiments are compared and thoroughly discussed. The lack of numerical results in the literature and the complexity of obtaining a closed form solution for the free vibrational characteristics of an oblate spheroid oblige us to seek alternative approaches for justifying the feasibility of the theoretical methods used in this paper. Eventually, these methods are general and may be used for any physical and geometrical parameters of the oblate spheroid. Therefore, the natural frequency for a thin sphere which is considered as an ultimate shape of the oblate spheroid may be determined by using these methods and the results are compared with the literature.

Table (1) shows the natural frequency of the three first axisymmetric modes of a full thin sphere. These frequencies were obtained from applying the direct analytical solution (DAS) [**Tavakoli, 1989**], the state space method (SSM) [**Tavakoli, 1989**], the finite element method (FEM) [**Tavakoli, 1989**] where a forty elements axisymmetrical model was used, Rayliegh method (RM) [**Fawaz, 1990**], and the method derived in this paper, namely the Rayleigh – Ritz method (RRM). The results of the latter method was obtained by setting the

4313

eccentricity ratio to zero in equation (7). Also it can be seen that the Rayleigh–Ritz's method predicts frequencies higher than the other methods given in the table. This fact is inherited to this method for its higher bounds prediction. However, it may be stated from this table that the two methods of solution presented in this work are dependable and may be used for other shell geometrical and physical parameter.

The experimental and theoretical frequencies for oblate shell are presented in table (2), this table indicates that the theoretical results by the Rayliegh and Rayleigh – Ritz's method predict frequencies higher than of the experimental. This is inherited to this particular method.

Figures (4) and (5) show the non–dimensional natural frequencies $\left(\lambda = \sqrt{\rho / E} \, \omega . a \right)$ of the first two modes of vibration as functions of the eccentricity ratio (which is one of the main indices of an oblate spheroid) obtained by the Rayleigh Ritz's method and the Rayleigh's method using the non – shallow shell theory. These figures show clearly the tendency of the natural frequencies towards lower values as the eccentricity increases. Also it is indicated that the curve obtained by the Rayleigh's method, adjoin to that obtained by the Rayleigh's – Ritz's method, although with slightly higher value, until the eccentricity reaches (0.6) where the Rayleigh's method curve start to diverge. Larger divergence occure at eccentricities higher than (0.9).

This behavior could be explained by the fact that the mode shapes of a closed spherical shell would resemble those of an oblate spheroid up to certain eccentricity. As the eccentricity increases, the oblate spheroid tends to flatten up. Such "flattening" causes the uncoupling of the radial (or transverse motion) and the tangential motion where the latter is minimized and the radial or transverse motion mode shape approaches that of a circular plate. Another reason is that the spherical shape is stiffer than the oblate spheroid due to the flattening in the geometry.

However, the sudden deviation in the curve predicted by (RM) for eccentricity larger than (0.6) may be considered due to additional constraints resulting from the deviation from the true mode shape. This causes higher values for the potential energy in Eq. (7) and thus the values of the natural frequencies diverge abruptly at higher values of eccentricity. This mean that the value predicted by the (RM) for eccentricities larger than (0.6) are in tremendous error and cannot be used.

Figure (6) gives the first few natural frequencies as function of the thickness ratio for an oblate spheroid with (e = 0) obtained by RRM. However, Fig. (7) shows the same results as given by [Kraus], for complete sphere. The two figures are in good agreement and justify very well the validity of the method used in this paper.

Figure (8) show the first few frequencies as functions of thickness ratio with (e = 0.6). All these figures are for (υ = 0.3) and they show the bending as well as the membrane modes using the non – shallow shell theory. It can be noted that the variation of the natural frequency of the bending modes increases with thickness and with the mode number. This phenomenon can be elaborated due to the fact that the strain energy increased with increasing the thickness ratio. Also, for larger eccentricity ratio, the variations are more pronounced than for smaller eccentricity.

For further illustration of the effect of thickness on the bending modes, Figure (9) shows the first two bending modes of an oblate spheroid with an eccentricity of (0.3) for several thickness ratios, obtained by applying the RM and RRM. It is well indicated that the figures obey the previous observation of the effect of thickness on bending modes.

Figures (10) and (11) illustrate the boundaries of the first three bending modes and the first membrane mode respectively with increasing the eccentricity (e). It may be observed from figure (10) that as the eccentricity increased, the natural frequency slowly decrease until reaching close to (0.5) where steeper variation occurs and the three curves

converge to very close values. On the other hand, Fig. (11) shows other features concerning the behavior of the first membrane mode with increasing eccentricity ratios.

From Fig. (12) it is concluded that the main features of the mode shapes associated with the first three natural frequencies rest in the number of the nodal lines in the upper and the lower shell parts. The number of these nodal lines is related to the order of the associated natural frequency.

CONCLUSIONS:

From the results obtained, the following conclusions may be drawn;

- The Rayliegh – Ritz method predict fairly well the natural frequencies of an oblate spheroidal shell for all values of eccentricities.
- Bending modes natural frequencies tend to decrease with increasing eccentricity ratio.
- Membrane modes natural frequencies tend to increase with increasing eccentricity ratio.

REFERENCES:

- Antoine Chaigne, Mathieu Fontaine, Oliver Thomas, Michel Ferre, Cyril Tou., "Vibrations of Shallow Spherical Shells and Gongs", J. of Sound and Vibration, 2002.

- Chang Y. C. and Demkowicz L., "A stability Analysis Vibrating Viscoelastic Spherical Shells", J. Appl. Math., Vol. 2(2), PP. 213 – 242, 1998.

- Fawaz Abbas Najim, "An Investigation into the Free axisymmetric vibration characteristics of isotropic thin oblate spheroidal shells", M. Sc. Thesis, Mechanical Engineering/ University of Baghdad, 1990.

- Haym Benaroya, "Mechanical Vibration", Prentice – Hill, Inc., U.S.A., 1998.

- Kalnins A., "Effect of bending on vibrations of spherical shells", J. Acoust. Soc. Amer., Vol.
- 36 (1), PP. 74 – 81, 1964.

- Kraus H., "Thin elastic shells", John Wiley and Sons, New York 1967.

- Nawal H. A. , " Theoretical Investigation of the Axisymmetric Free Vibration of An Oblate Spheroid Shells", M. Sc. Thesis, Mechanical Engineering/ University of Babylon, 2005.

- Penzes L. and Burgin G.," Free vibrations of thin isotropic oblate spheroidal shells", General Dynamic Report No. GD/C–BTD 65 – 113, 1965

- Penzes L., " Free vibrations of thin orthotropic oblate spheroidal shells", J. Acoust. Soc. Amer., Vol. 45, pp. 500 – 505, 1969.

- Tavakoli M. S. and Singh R., "Eigensolutions of joined / hermetic shell structures using the state space method", J. Sound and Vibration Vol. 100, PP. 97 – 123, 1989.

- Wilfred E. Baker " Axisymmetric modes of vibration of thin spherical shell", J. Acoust. Soc. Amer., Vol. 33, PP. 1749 – 1758, 1961.

Table (1) : Natural frequencies of the first three axisymmetric modes of thin sphere, Hz.
r = 0.1143 m , h = 0.0057 m , E = 207 Gpa , ρ = 7800 Kg/m^3 , υ = 0.3

n	m	DAS.[1]	SSM.[2]	FEM.[3]	R.M.[4]	RRM.[5]	δ_1%	δ_2%	δ_3%	δ_4%
							Differences with respect to DAS. %			
0	2	5281	5291	5383	5335	5315	- 0.2	≈ 0.0	-1.0	-0.6
0	3	6321	6330	6319	6510	6513	- 0.1	≈ 0.0	-3.0	-3.0
0	4	6883	6894	6875	--------	6950	- 0.1	0.1	-----	-1.0

(1) Direct Analytical Solution [4] δ_1% = (DAS – SSM) / DAS * 100
(2) State Space Method [4] δ_2% = (DAS – FEM) / DAS * 100
(3) Finite Element Method [4] δ_3% = (DAS – R M) / DAS * 100
(4) Rayleigh Method [5] δ_4% = (DAS – RRM) / DAS * 100
(5) Rayleigh – Ritz Method [*present work*]

Table (2) : Theoretical and experimental natural frequencies
of thin oblate shell (e=0.683)
Hz.
a=0.185m , b=0.135m , h= 0.0015m , , E = 68 Gpa , $\rho = 2720 Kg/m^3$, $\upsilon = 0.3$

	Theoretical			Differences with respect to Expt. ٪	
	RRM	RM[5]	Expt. [5]	δ_1٪	δ_2٪
ω_1	2517	3110	2400	-4.87	-29.58
ω_2	2973	3378	2600	-14.34	-29.92
ω_3	3086	....	2900	-6.41	....
ω_4	3180	....	3100	-2.58	....

δ_1٪= (Expt. – RRM) / Expt. * 100

δ_2٪= (Expt. – R M) / Expt. * 100
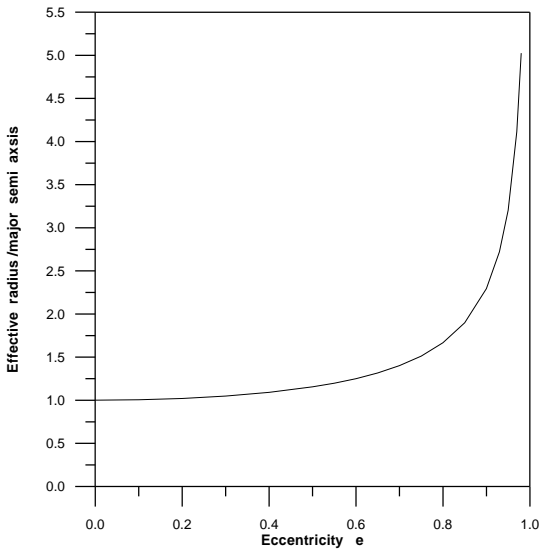
Fig. (2) The effective radius / major semi Φ_o) of the – axis vs. eccentricity vs.
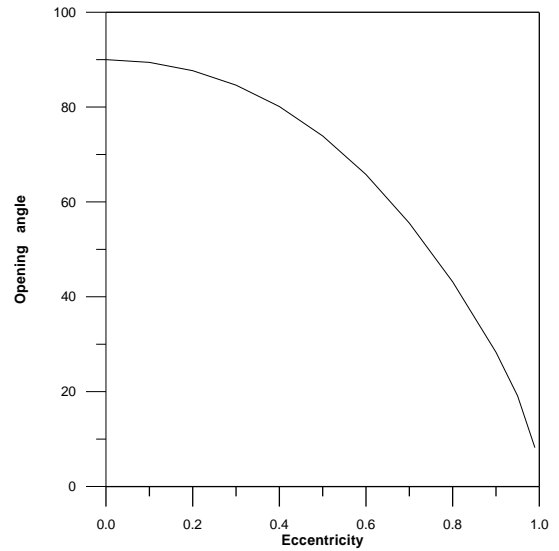
Fig. (3) : The opening angle (approximate spherical shells eccentricity.
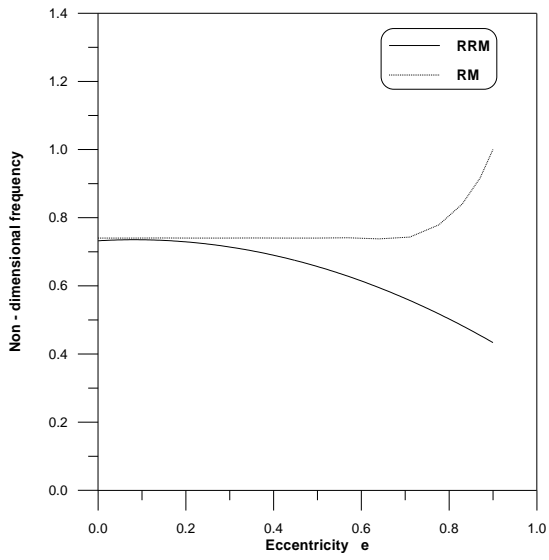
Fig. (4): A comparison between RM and RRM results
             showing the effect of eccentricity on the first
             bending mode of vibration
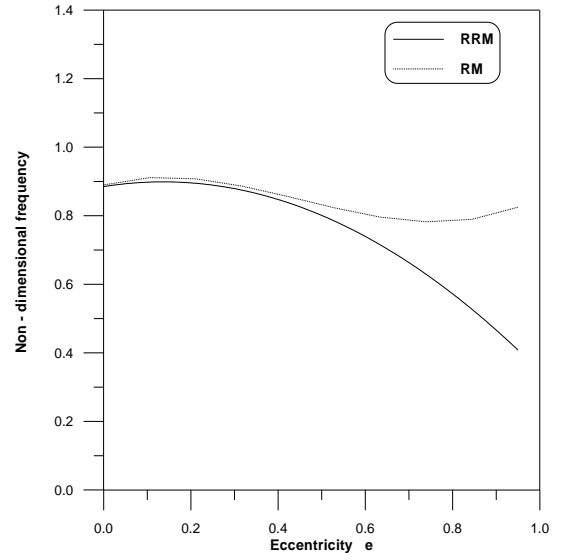
Fig. (5) :A comparison between RM and RRM results
            showing the effect of eccentricity on the second
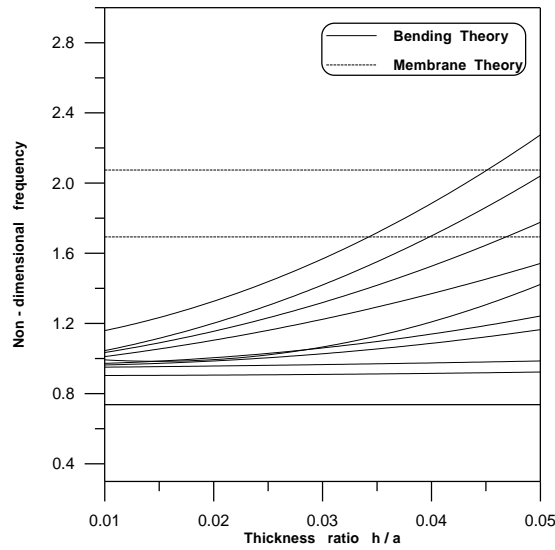   bending mode of vibration

Fig. (6): Effect of the thickness ratio on the natural
            frequencies of a full sphere or an oblate
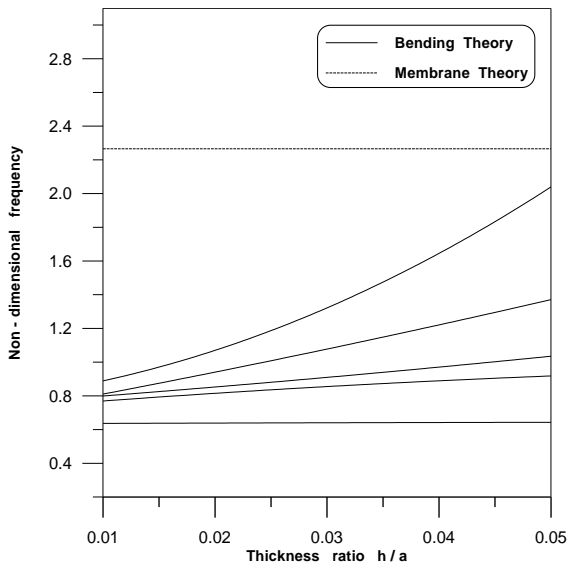   spheroidal shell (e = 0) obtained by RRM

Fig. (7): Effect of the thickness ratio on the natural
frequency   of   an   oblate   spheroidal   shell
(e = 0.6) obtained   by   RRM
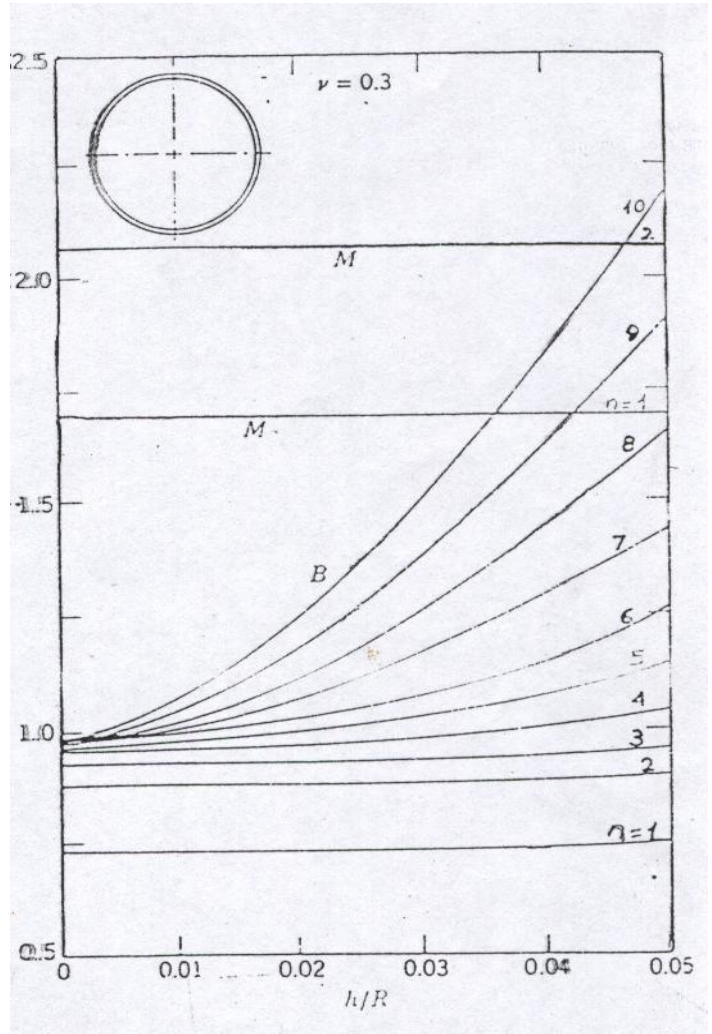
Fig. (8): Effect of the thickness ratio on   the   natural
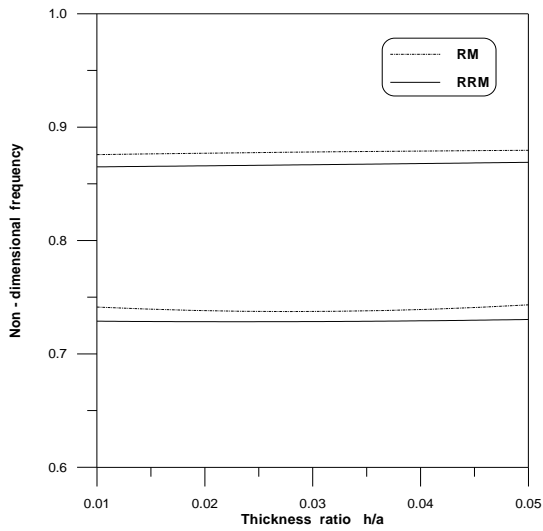frequencies   of   a   full   sphere   extracted   from
[11]

Fig. (9): Effect of thickness ratio on the first and second bending modes of an oblate spheroidal shell (e = 0.3)
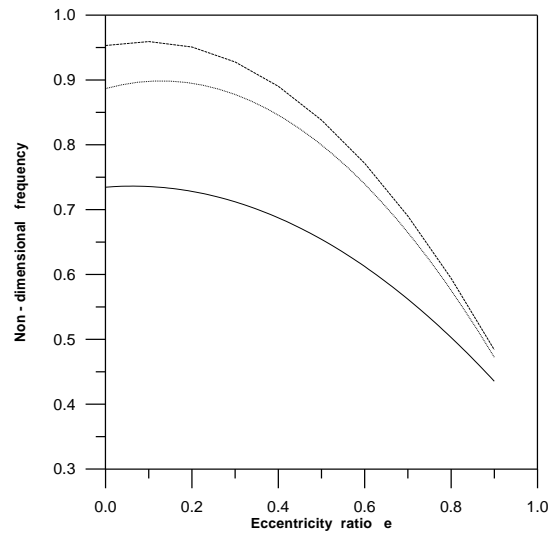

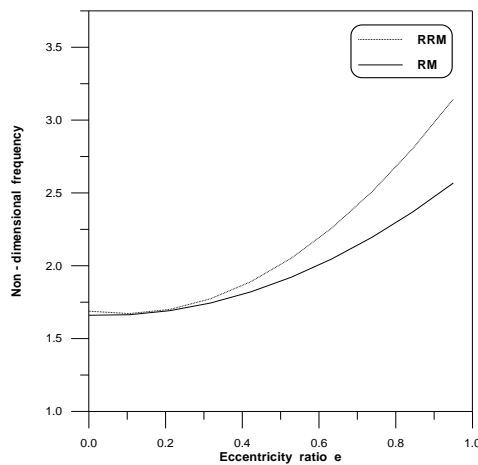Fig. (10): Effect of eccentricity on the three first bending modes obtained by RRM

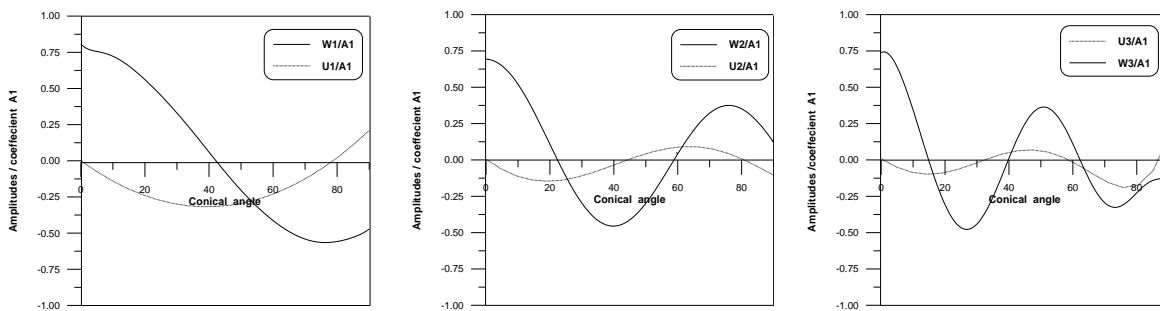Fig. (11): Effect of eccentricity on the first membrane modes

Fig. (12): Normalized mode shape associated with the first three natural frequency of non – shallow spheroidal shell (e = 0.683) obtained by RRM